



# A model for length control of flagellar hooks of *Salmonella typhimurium*

J.P. Keener\*

Department of Mathematics, University of Utah, 155 South 1400 East, Salt Lake City, UT 84112, USA

Received 12 July 2004; received in revised form 16 November 2004; accepted 18 November 2004

## Abstract

We present a mathematical model for the growth and length regulation of the hook component of the flagellar motor of *Salmonella typhimurium*. Under the assumption that the molecular constituents are translocated into the nascent filament by an ATP-ase and then move by molecular diffusion to the growing end, where they polymerize into the growing tube, we find that there is a detectable transition from secretion limited growth to diffusion limited growth. We propose that this transition can be detected by the secretant FliK, allowing FliK to interact with FlhB thereby changing the secretion target of the type III secretion machinery and terminating the growth of the hook.

© 2005 Elsevier Ltd. All rights reserved.

Keywords: ■; ■; ■

## 1. Introduction

The flagellar motor of *Salmonella typhimurium* is morphologically divided into three primary parts: the basal body, the hook, and the filament (see Fig. 1). The filament and hook are external to the cell, while the basal body is anchored in the inner and outer membranes. The filament is the largest portion of a flagellum, stretching to more than 10 μm, and when rotated by the motor at the base, serves as a propeller. The hook lies between the filament and the basal structure and works as a universal joint. The hook is flexible, but torsionally rigid, whereas the filament is a rigid helical structure.

The synthesis of the flagellar motor requires the expression of 50 genes, arranged in clusters of 17 operons, in a carefully controlled temporal order. These operons are divided into three classes according to their order of expression Kutsukake et al. (1990). The master operon in the highest class governs the expression of the

rest by activating operons in the second class. A flagellum-specific sigma factor in the second class regulates the expression of other operons in the same or lower classes. Significantly, the basal structure and hook must be complete before the genes for the filament are expressed.

Assembly of the flagellum begins with the insertion of a ring structure within the cytoplasmic membrane. When this ring structure is completed, a secretion apparatus is constructed and inserted. The secretion apparatus is needed for export of flagellar structural subunits beyond the inner cytoplasmic membrane. Beyond the cytoplasm, secreted subunits self-assemble into the growing structure.

The basic mechanism of construction of the flagellum is as follows. The nascent flagellum, a hollow cylindrical structure (outer diameter 20 nm, inner diameter 2 nm (Yonekura et al., 2003)), is formed when partially unfolded monomeric constituents reach the growing tip and polymerize. The monomeric subunits are secreted from the cellular cytoplasm following hydrolysis of ATP by the ATP-ase protein FliI. Secretion of the hook constituent protein, FlgE, proceeds until the

\*Tel.: +1 801 581 6089; fax: +1 801 585 1640.

E-mail address: keener@math.utah.edu (J.P. Keener).

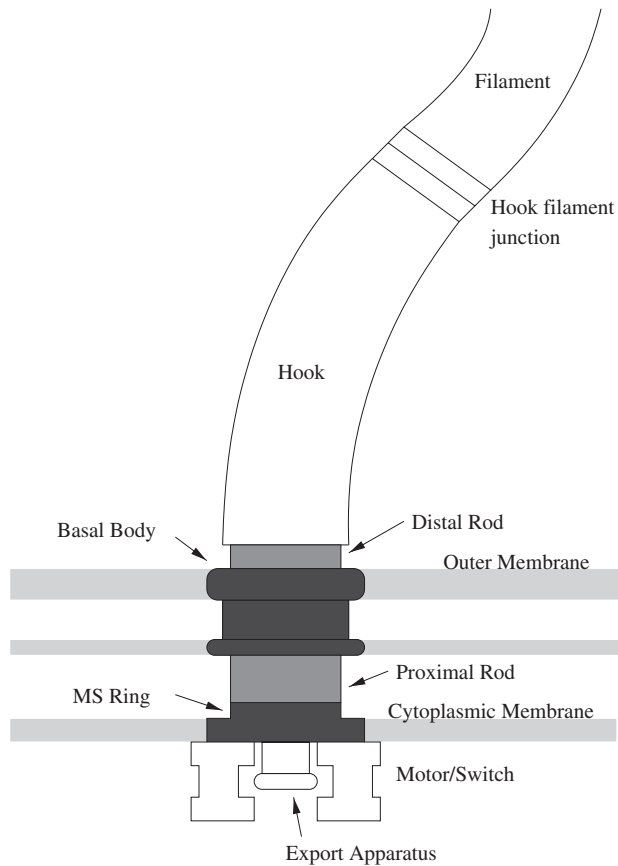


Fig. 1. Schematic diagram of flagellar motor construction.

hook is  $55(\pm 9)$ nm long. At that point, secretion switches to proteins FlgK and FlgL which form the hook-filament junction (Table 1) and then secretion of FliC, the filament constituent protein (flagellin), begins.

The mechanism for the control of hook length is not known. However, hook length is believed to be controlled by the protein FliK. It is believed that FliK functions together with a membrane associated protein of the export apparatus, FlhB, to mediate switching of export substrate specificity, from hook protein to flagellin, upon completion of hook assembly (Minamino et al., 1999). In wild-type cells, hooks are tightly regulated to be  $55 \pm 9$  nm, whereas in FliK mutants, hooks are extraordinarily long (polyhooks), and there is no filament extension from the hook. Conversely, when FliK is overexpressed, hooks are somewhat shorter ( $46 \pm 7$  nm), while when FliK is underproduced, hooks are longer with substantially more variation ( $75 \pm 46$  nm) (Muramoto et al., 1998) (see Fig. 2). FliK is known to be secreted during the hook-growth phase. In FliK mutants (polyhook phenotype), no FliK is found in the extracellular medium, indicating that secretion of FliK is a crucial part of the hook-length regulation. FliK is secreted most efficiently before hook completion and a decrease in the secretion efficiency of FliK results in polyhooks (Minamino et al., 1999).

Table 1

Some proteins used in hook/filament construction and their function

Protein	Function
FliC	Filament constituent protein
FlgE	Hook constituent protein
FlgD	Hook cap protein
FlgKL	Hook-filament junction
FliK	Hook length protein
FliI	Secretion ATP-ase
FlhB	Secretion target protein

A verbal model for the control of hook length has been proposed (Muramoto et al., 1998). Their idea is that the export of FlgE occurs in three distinct stages. In stage 1, secretion by the ATP-ase is rate limiting so that there is no more than one monomeric subunit in the forming channel at any given time. In stage 2, the increased hook length has caused diffusion to slow so that it is rate limiting and there are several hook subunits in the channel causing interference in the diffusion process. In stage 3, the channel is completely congested and secretion export is coupled to assembly at the distal end. This coupling causes a delay in the ATP-ase transport cycle, allowing the length control protein FliK to bind a special binding site on the export apparatus, leading to a change of the specificity of the transporter.

The main purpose of this paper is to explore this verbal explanation using mathematical models. Although this verbal model cannot be correct in its details, we find support for the idea that there is a switch between secretion-limited growth (stage 1) and diffusion limited growth (stage 2) which may be detected by the secretant FliK.

In what follows we describe three models for the interaction between secretion and diffusion. The first treats diffusion and secretion in a simplistic but suggestive way. The second examines the movement of monomer in a probabilistic way using a Langevin formulation. The third examines the stochastic process using a Fokker-Planck formulation. All three of these show transitions in which there is a qualitative and quantitative change in the way in which translocation of the secretant molecule takes place. This, we propose, could be the length-detection signal. We know of no data directly supporting or contradicting this hypothesis.

## 2. Diffusion through a hollow tube

Our first step is to develop a simple model that contains the essential ideas. Later models will focus on some of the details that are ignored here.

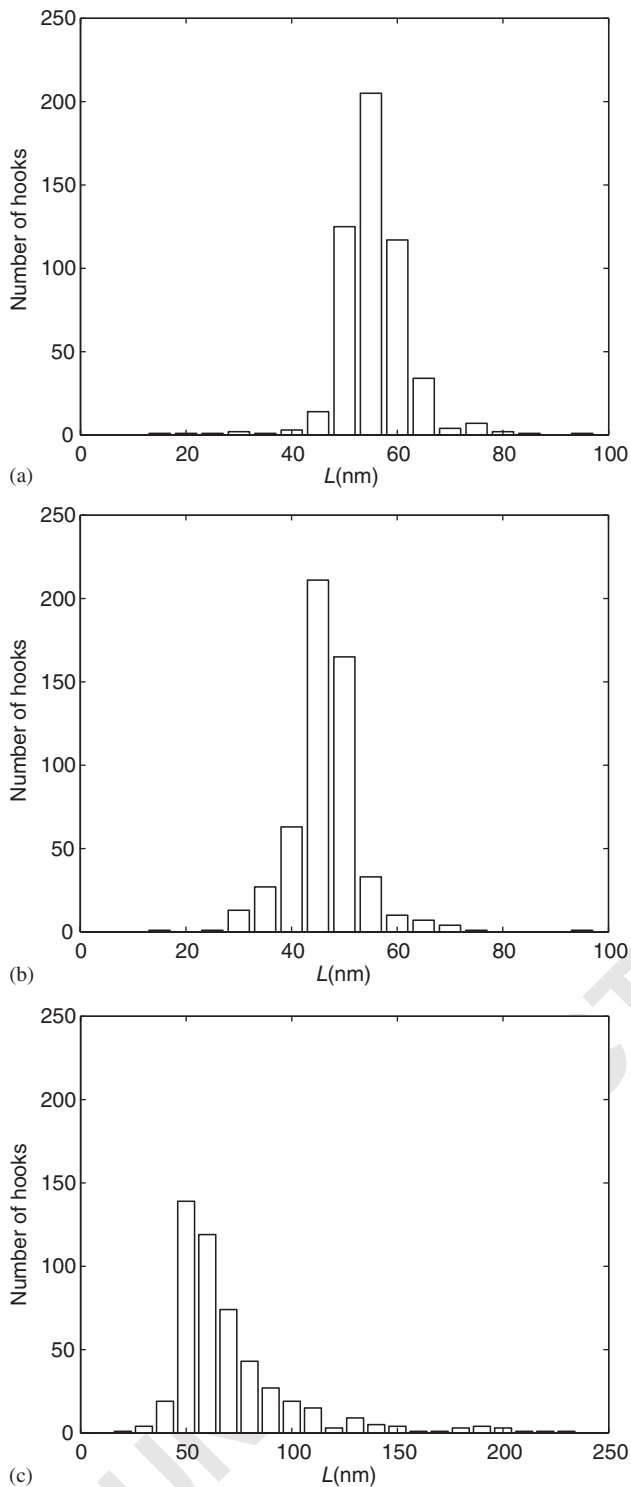


Fig. 2. Hook length distribution for (a) wild type, (b) when FliK is overproduced, and (c) when FliK is underproduced. Redrawn from Muramoto et al. (1998).

The growth process involves three molecular processes (Fig. 3). The monomeric subunit is first secreted into the cytoplasmic end of the filament, it moves

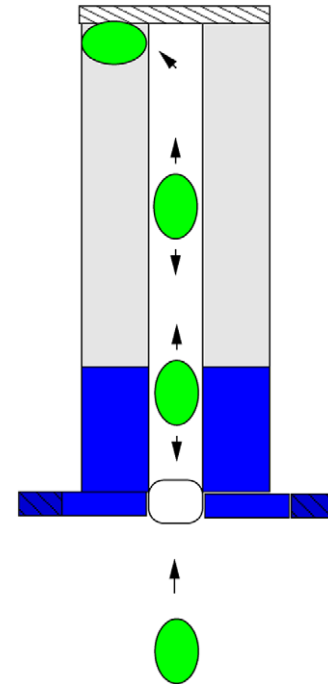


Fig. 3. Schematic diagram of hook and filament growth process. Monomeric subunits are secreted into the cytoplasmic end of the nascent filament, they move by diffusion to the capped end where they are folded into the growing end.

diffusively along the tube and is then enfolded into the growing end.

An important fact is that the nascent tube has an inner diameter of about 2 nm, which for steric reasons, means that movement of molecules must be in single file, with no passing permitted (Macnab, 2003). Thus, the concept of a molecular concentration is not useful here. Rather, we let  $p(x, t)$  be the probability that at time  $t$  there is a molecular subunit between position  $x$  and  $x + l$ , where  $l$  is the length of the monomeric unit, along the forming tube with length  $L(t)$ . Standard conservation implies that

$$\frac{\partial p}{\partial t} = -\frac{\partial J}{\partial x}, \quad (1)$$

where  $J$  is the flux of probability.

For a standard diffusion process,  $J = -D \frac{\partial p}{\partial x}$ . There is no difference between a one-dimensional diffusion process and a single-file diffusion process, unless individual molecules are marked and their motion followed. It is useful to note that if  $l$  represents the length of a monomeric subunit, then  $\frac{J}{l}$  is the flux of numbers of molecules per unit time.

At the polymerizing end of the hook, there is a cap constructed of the protein FlgD. This protein is thought to prevent the escape of FlgE and to facilitate polymerization (Hughes and Aldridge, 2001). It follows that at the growing tip the flux of molecules must exactly

match the rate of polymerization. Thus, at  $x = L$

$$\frac{J}{l} = k_p p, \quad (2)$$

where  $k_p$  is the rate constant for polymerization.

The secretion process is energized by an ATP-ase (FliI). It is not known exactly how this ATP-ase works, although there are hypothetical verbal models. One proposal (Minamino and Macnab, 2000) is that soluble FliI (complexed with FliJ) receives the export substrate from cytoplasmic chaperones, and delivers them to a membrane associated structure, which then translocates them to the channel in the nascent structure.

To model this process, we assume that the membrane associated structure can be in one of two states, either empty awaiting binding with its cognate substrate, or bound and involved in translocation. It follows that the probability of going from the unbound to the bound state in time  $\delta t$  is  $K_{on}\delta t = k_{on}\frac{[S]}{K_s+[S]}\delta t$ , where  $[S]$  is the concentration of the substrate. Usually, we would assume that the probability of going from the bound to unbound state is  $k_{off}\delta t$ , however, because of the steric no-passing condition, translocation and unloading cannot take place unless there is open space for the subunit to move into. Thus, we assume that the probability of going from the bound to the unbound state is  $k_{off}(1-p(0))\delta t$ . If  $P$  is the probability that the membrane associated ATP-ase is bound by its cognate substrate  $S$ , then

$$\frac{dP}{dt} = K_{on}(1-P) - k_{off}(1-p(0))P, \quad (3)$$

where  $p(0)$  is the probability that the  $x = 0$  end of the nascent hook is occupied at time  $t$ . The primary consequence of this statement is that translocation can be delayed if the forming hook is crowded with monomer. With these as the binding and unbinding rates, the flux of monomer must be the same as the unbinding rate,

$$\frac{J}{l} = k_{off}(1-p(0))P. \quad (4)$$

The length  $L(t)$  of the growing hook or filament is governed by the differential equation

$$\frac{dL}{dt} = \frac{J}{\beta l}, \quad (5)$$

at  $x = L$ , where  $\beta$  is the number of monomers per unit length of hook ( $\beta = 2.1/\text{nm}$ ).

The full time dependent solution of this problem requires that we solve the diffusion equation

$$\frac{\partial p}{\partial t} = -\frac{\partial J}{\partial x}, \quad (6)$$

subject to boundary conditions (2) at the moving boundary  $x = L$ , and (3), (4) at  $x = 0$ . This is a free boundary problem whose solution requires numerical

simulation. However, simulations show that an extremely good approximate solution can be found by taking the diffusion equation to be in steady state. (A more precise mathematical justification of this approximation can also be given, but is not particularly relevant to this discussion.) For this, solutions satisfy

$$J = -Dp_x \quad (7)$$

with  $J$  independent of  $x$  (but slowly varying in time). It follows that

$$J = \frac{D}{L}(p(0) - p(L)). \quad (8)$$

Furthermore, we take  $P$  to be in steady state, so that

$$P = \frac{K_{on}}{K_{on} + k_{off}(1-p(0))}. \quad (9)$$

With this simplification, (4) becomes

$$\frac{J}{l} = k_{off}K_{on}\frac{1-p(0)}{K_{on} + k_{off}(1-p(0))}. \quad (10)$$

Finally, boundary condition (2) becomes

$$p(L) = \frac{1}{k_p} \frac{J}{l}. \quad (11)$$

The analytical solution of these equations is readily obtained. From Eq. (10), we find that

$$p(0) = 1 - \frac{K_{on}}{k_{off}} \frac{\frac{J}{l}}{(K_{on} - \frac{J}{l})} \quad (12)$$

and  $p(L)$  is determined from Eq. (11), so that from Eq. (8),

$$\frac{Ll}{D} = \frac{l}{J} - \frac{K_{on}}{k_{off}} \frac{1}{(K_{on} - \frac{J}{l})} - \frac{1}{k_p}, \quad (13)$$

yielding a relationship between length  $L$  as a function of flux  $J$ . In dimensionless variables this is

$$\lambda = \frac{1}{j} - \frac{K_a}{1-j} - K_b, \quad (14)$$

where  $\lambda = \frac{LlK_{on}}{D}$  is the dimensionless length, and  $j = \frac{J}{lK_{on}}$  is the dimensionless flux. The solution is controlled by the two non-dimensional parameters  $K_a = \frac{K_{on}}{k_{off}}$  and  $K_b = \frac{K_{on}}{k_p}$ . Recall that the velocity of growth  $\frac{dL}{dt} = V$  satisfies  $\beta V = \frac{J}{l}$ .

While it is possible to solve for  $J$  as a function of  $L$  (using the quadratic formula), this is not especially illuminating. Instead, it is easier to plot this relationship for several different parameter values.

In Fig. 4 are shown plots of dimensionless flux  $j$  as a function of dimensionless length  $\lambda$  for several values of the parameter  $K_a$  and  $K_b = 0$ . Notice that increasing  $K_b$  merely shifts the  $j$ - $\lambda$  curve to the left.

These flux-length curves exhibit reasonable qualitative behavior. Iino (1974) found velocity-length curves for filaments to be well fit by exponentials for filaments in the range of 4–12  $\mu\text{m}$ , and (Koroyasu et al., 2003) found

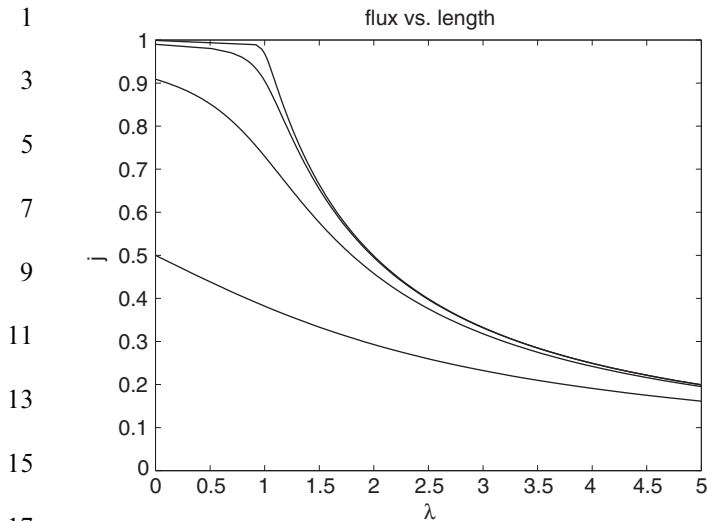


Fig. 4. Dimensionless flux  $j$  as a function of dimensionless length  $\lambda$  for  $K_a = 1, 0.1, 0.01, 0.001$  (bottom to top) from Eq. (14).

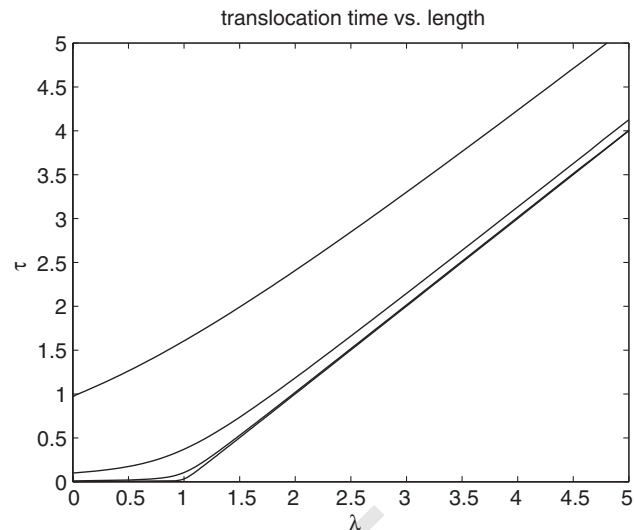


Fig. 5. Dimensionless translocation time  $\tau$  as a function of dimensionless length  $\lambda$  for  $K_a = 1, 0.1, 0.01, 0.001$  (top to bottom) from Eq. (14).

that hook growth velocity could be approximated by a decaying exponential leading to a constant rate of growth for polyhooks in the range of 60–900 nm. While the relationship (14) is not exponentially decreasing, it shows monotonic decay as a function of length. More important, for small values of  $K_a$ , the curves are “biphasic” with a plateau for small lengths preceding rapid decay. The biphasic nature of these curves for small  $K_a$  reflects two phases of growth. When the length is small, the rate limiting step is substrate binding since diffusion out of the nascent tube is rapid and uninhibited. When the length is large, diffusion is rate limiting and secretion is restricted by the need for space into which the secreted molecule can be released.

The consequences of this plateau is made more explicit by examining the translocation time for each monomer,

$$T = \frac{l}{J} - \frac{1}{K_{on}}, \quad (15)$$

or in dimensionless units

$$\tau = \frac{1}{j} - 1, \quad (16)$$

where  $\tau = K_{on}T$  is the dimensionless translocation time.

In Fig. 5 are shown several plots of the dimensionless translocation time as a function of dimensionless length. Here the translocation time decreases as  $K_a$  decreases, indicating that less time is spent in translocation than in docking as  $K_a = \frac{K_{on}}{k_{off}}$  decreases. In the limit that  $K_a \rightarrow 0$ , there is a sharp transition between zero time spent in translocation and a linear increasing translocation time as a function of length. This transition occurs at  $\lambda = 1 - K_b$ .

### 3. Stochastic models of translocation

#### 3.1. Langevin formulation

While the previous model is interesting in that it gives credence to the idea that there could be a length-dependent transition in translocation time, leading to a length-dependent switching signal, the model is seriously flawed in its details. The difficulty is that in the model, monomers are described mathematically as diffusing points, when in fact they are quite long. FliK is 405 and FlgE is 402 residues long. It is uncertain how long they are in their partially unfolded state in the growing hollow tube, but if they are temporarily alpha-helical, they would be on the order of 75 nm long. This is obviously as long or longer than the hook structure that is being built.

To include this important feature in the model, we assume that the location of monomers can be described by their endpoints,  $x_j$  and  $y_j$ , where  $x_j$  is the leading edge and  $y_j$  is the trailing edge, respectively, of the  $j$ th monomer. These endpoints are coupled by a massless, linear spring with neutral length  $l$ , and the monomers move diffusively through the one dimensional channel. This model is depicted in Fig. 6.

As long as they are within the tube (i.e.  $0 < x_j, y_j < l$ ), their positions can be described by the stochastic differential equations (Bird et al., 1987)

$$\begin{aligned} \frac{v}{2} dx_j &= k(y_j - x_j + l) dt + \sqrt{vk_B T} dt \xi_j, \\ \frac{v}{2} dy_j &= k(x_j - y_j - l) dt + \sqrt{vk_B T} dt \eta_j, \end{aligned} \quad (17)$$

where  $\xi_j$  and  $\eta_j$  are independent  $N(0,1)$  random variables, and it is required that  $y_j > x_{j+1}$ . It follows

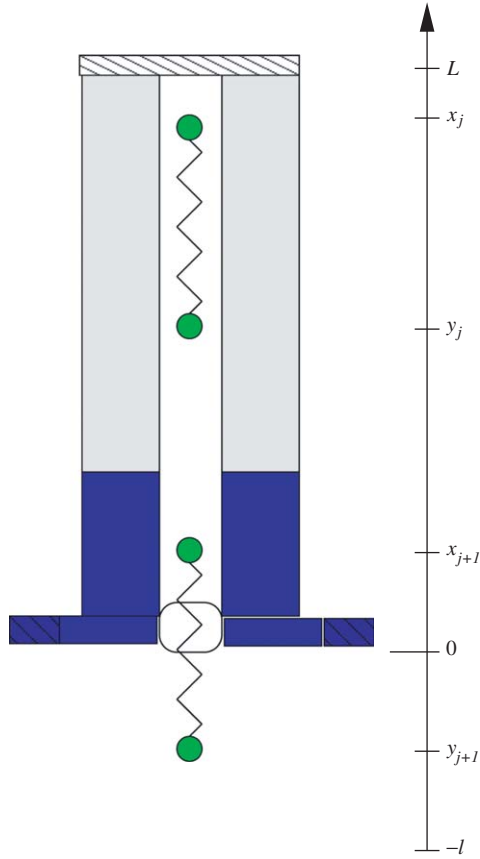


Fig. 6. Depiction of 1-D spring model for monomer diffusion through the hollow tube.

that the diffusion coefficient for each monomer is  $D = \frac{k_B T}{\nu}$ .

The boundary conditions for this model must also be specified. We assume that at the growing end ( $x = L$ ), the folding of the monomer provides a force which opposes its motion back into the tube. That is, if  $x_j > L$ ,

$$\frac{v}{2} dx_j = (k(y_j - x_j + l) dt + F_f dt + \sqrt{\nu k_B T} d\zeta_j), \quad (18)$$

where  $F_f$  is the force on the monomer due to folding. Once  $y_j > L$ , the  $j$ th monomer has completely exited the tube and so can no longer interact with the next molecule  $x_{j+1}$ .

A similar restriction is appropriate at the secretion end ( $x = 0$ ). Here the threading of the monomer into the tube is enhanced by the ATP-ase, although the exact mechanism is not known. For modeling purposes, we assume that the secretion is by a brownian ratchet mechanism, in which there is a positive secretion force  $F_s$  pushing the monomer into the tube. That is, for  $-l < y_j < 0$  the stochastic differential equation for  $y_j$  is given by

$$\frac{v}{2} dy = k(x_j - y_j - l) dt + F_s dt + \sqrt{\nu k_B T} d\eta_j, \quad (19)$$

where  $F_s l = N \Delta G$  with  $\Delta G$  the free energy of ATP hydrolysis, and  $N$  the (unknown) number of ATP molecules that are hydrolyzed for each secreted monomer.

It is important to note that  $L$  is the length of the hollow tube, from the cytoplasm to the end of the hook, and this includes the basal body. The width of the basal body is not known precisely, but it is probably in the range of 25–35 nm.

Finally, there is the question of how to initiate secretion. Here we assume that the  $j + 1$ st molecule binds (and secretion begins) via a Poisson process with binding rate  $\lambda$ , as long as the secretion site is available,  $y_j > 0$ .

In Fig. 7 is shown an example of particle paths for this stochastic process. The distance along the tube is in units of  $l$ , the monomer length, and the tube length for this simulation is  $L = 1.5l$ . Other parameter values are listed in Table 2.

In this simulation, secretion was initiated at times 0, 0.3220, 0.3580, 0.5340, 0.9540, and 0.9910 s. The secretion of monomers 2 and 5 (at  $t = 0.3220$  and  $t = 0.9540$  s) was unhindered by other monomers in the tube, but the secretion of monomers 1, 3, and 4 was

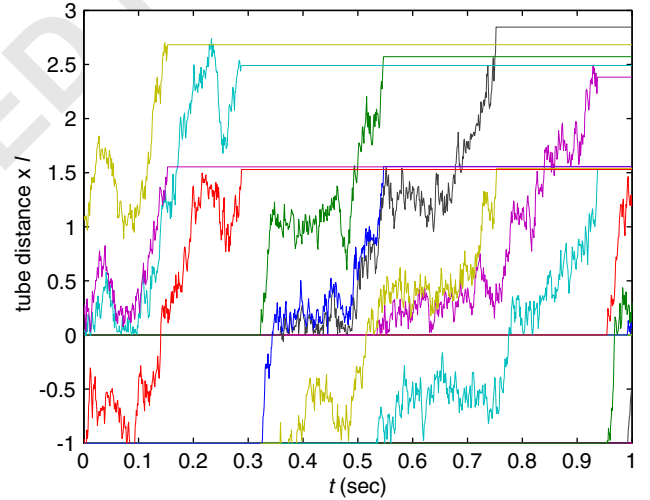


Fig. 7. Depiction of Langevin simulation of secretion and diffusion of monomer.

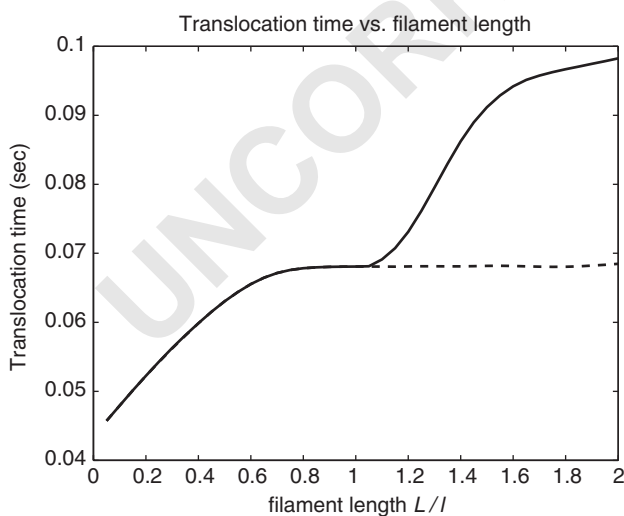
Table 2  
Parameter values for Fig. 7

$D$	$10^{-10} \text{ cm}^2/\text{s}$	105
$\lambda$	10/s	107
$\frac{F_s}{\nu l}$	25/s	109
$\frac{F_f}{\nu l}$	20/s	111
$\frac{k}{\nu l}$	250/s	
$\frac{v}{l}$	75nm	

1 significantly hindered by monomers that had been  
 2 previously secreted and were still in the tube, and  
 3 complete secretion of these monomers is noticeably  
 4 delayed.

5 The secretion/translocation time for a monomer is  
 6 governed by the interplay of three forces, the force of  
 7 secretion  $F_s$ , the force of folding  $F_f$ , and the force from  
 8 interference with other monomers in the tube. If the tube  
 9 is short, translocation is rapid since a monomer can be  
 10 simultaneously pushed by secretion and pulled by  
 11 folding. However, if the tube is longer than the length  
 12 of the unfolded monomer, it cannot be simultaneously  
 13 pushed and pulled, and there can also be monomers  
 14 contained completely in the tube that hinder its  
 15 secretion.

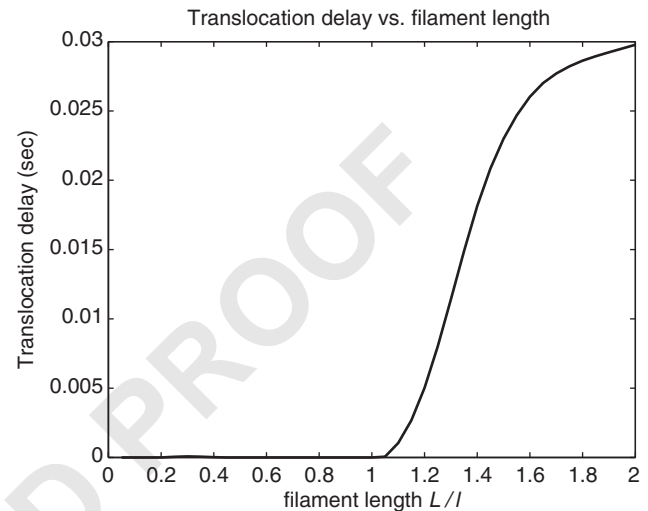
16 The average translocation time is an increasing  
 17 function of tube length. In Fig. 8 is shown the  
 18 translocation time as a function of length with  
 19 parameter values as shown in Table 3. The dashed  
 20 curve in this figure shows the translocation time for  
 21 unhindered translocation. It is clear from this figure that  
 22 when  $\frac{L}{l}$  is small (less than 1), translocation is unhin-  
 23 dered, while when  $\frac{L}{l}$  (greater than 1), translocation is  
 24 hindered by the presence of other monomers in the tube.  
 25 In the first phase, with  $\frac{L}{l} < 1$ , the monomer is both  
 26 “pushed” by the ATP-ase and “pulled” by folding at the  
 27 polymerizing end. The amount of pulling during  
 28 secretion decreases as the length of the tube increases.  
 29 When  $\frac{L}{l} > 1$ , there is the possibility of a second monomer  
 30 being in the tube that hinders free secretion. This  
 31 hindrance leads to a noticeable increase in translocation  
 32 time as a function of  $L$ , as seen in Fig. 8. The sharpness  
 33 of this transition depends on parameter values and  
 34 becomes less sharp if diffusion is increased or if the  
 35 spring constant is increased.



36 Fig. 8. Translocation time from Langevin simulation plotted as a  
 37 function of  $\frac{L}{l}$ .

38 Table 3  
 39 Parameter values for Fig. 8

$D$	$10^{-11} \text{ cm}^2/\text{s}$	59
$\lambda$	5/s	61
$\frac{F_s}{v l}$	25/s	63
$\frac{F_f}{v l}$	20/s	65
$k$	50/s	67
$\frac{v}{l}$	75 nm	69



40 Fig. 9. Translocation delay due to interference with secretion plotted  
 41 as a function of  $\frac{L}{l}$ .

42 The feature of this curve that is most significant is the  
 43 translocation delay as a function of length, determined  
 44 as the difference between the hindered translocation  
 45 time and the unhindered translocation time. This  
 46 translocation delay is shown plotted in Fig. 9.

### 47 3.2. The mean translocation time

48 One of the disadvantages of the model used in the last  
 49 section is that, being a Langevin model, simulations to  
 50 find mean behavior are time consuming, making it  
 51 difficult to explore the behavior of the model for ranges  
 52 of parameter values. To explore this stochastic process  
 53 further, we examine more closely a simplified model for  
 54 which a Fokker–Planck formulation is possible. In  
 55 particular, we examine the situation in which there is an  
 56 unfolded molecule being secreted and there may be  
 57 another molecule inside the tubular flagellum that can  
 58 hinder secretion. We let  $y$  be the trailing position of a  
 59 molecule in the tube, and we let  $x$  be the leading edge of  
 60 the molecule that is being secreted.

61 We suppose that both particles diffuse, but that they  
 62 are not permitted to pass, so that  $x < y$ . We also assume

that  $x$  is not allowed to exit the tube at  $x = 0$ , and there is a Brownian ratchet “pushing” the secreted molecule. To model the exit of  $y$  from the end of the tube, we assume that there is standard brownian diffusion, as well as a brownian ratchet associated with folding pulling the molecule from the tube. This model is a simplification of the previous model in that here the unfolded molecules are rigid rods of fixed length  $l$ . The model is depicted by Fig. 10.

The Langevin equations for these two “particles” are

$$\begin{aligned} v dx &= F_s dt + \sqrt{2vk_b T} d\xi, \\ v dy &= F_f H(y - L + l) dt + \sqrt{2vk_b T} d\eta, \end{aligned} \quad (20)$$

where  $H(y)$  is the usual Heaviside function, used here to indicate that the force of folding is applied to the particle at  $y$  only if  $y > L - l$ .

Now we suppose that  $p(x, y, t)$  is the probability distribution function for the location of the particles  $x$  and  $y$  at time  $t$ . Associated with the velocities (20) there is the flux of probability  $J$  where

$$vJ = v \begin{pmatrix} J_x \\ J_y \end{pmatrix} = \begin{pmatrix} F_s \\ F_f H(y - L + l) \end{pmatrix} p - k_b T \nabla p. \quad (21)$$

The Fokker–Planck equation for the probability distribution  $p(x, y, t)$  is

$$\begin{aligned} v \frac{\partial p}{\partial t} &= -\nabla \cdot J \\ &= -\nabla \cdot \begin{pmatrix} F_s p \\ F_f H(y - L + l) p \end{pmatrix} + k_b T \nabla^2 p, \end{aligned} \quad (22)$$

defined on the domain  $R = \{(x, y) | x < y < L, 0 < x < l\}$ . The boundaries  $x = 0$  and  $x = y$  are reflecting so that  $J_x = 0$  at  $x = 0$ ,  $J_x = J_y$  on the line  $y = x$ . We are interested in determining the amount of time spent in

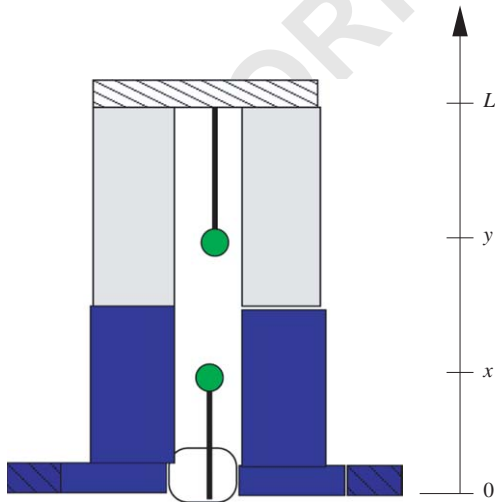


Fig. 10. Depiction of the two particle model for monomer diffusion through the hollow tube.

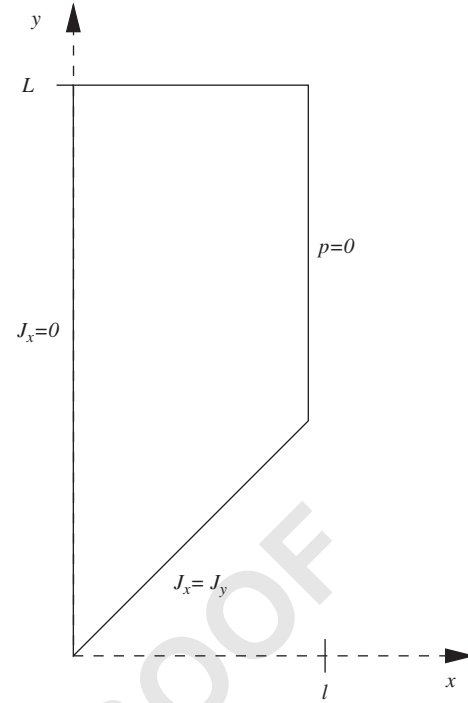


Fig. 11. Domain  $R$  and boundary conditions for the Fokker–Planck Eq. (22).

translocation (Fig 11). Thus, the boundary  $x = l$  is absorbing so that  $p = 0$  at  $x = l$ . The boundary condition at  $y = l$  is non-standard. If  $y = L$ , the leading molecule has left the tube and the motion of  $x$  is unimpeded, so that

$$v \frac{\partial p}{\partial t} = -(F_s p + F_f H(x - L) p)_x + k_b T p_{xx}, \quad (23)$$

for  $y = L$ . Notice that if  $L < l$ , the molecule with leading end at  $x$  can simultaneously feel the effects of secretion and folding. Notice, also, that if  $L < l$  the domain  $R$  is the triangular region  $\{(x, y) | x < y < L, 0 < x < l\}$  together with the line  $y = L, 0 < x < l$ , part of which is not on the boundary of the triangular domain.

We wish to determine the mean exit time for  $x$  across the boundary  $x = l$ . From standard arguments (Gardiner, 1985) (see Appendix), the mean exit time for this process starting from position  $x$  and  $y$  is given by  $S(x, y)$  where

$$-v = \begin{pmatrix} F_s \\ F_f H(y - L + l) \end{pmatrix} \cdot \nabla S + k_b T \nabla^2 S, \quad (24)$$

subject to the boundary conditions  $S = 0$  if  $x = l$  and  $n \cdot \nabla S = 0$  if  $x = 0$ , or  $x = y$ , where  $n$  is the outward unit normal vector. To specify the remaining boundary condition, observe that if  $y = L$ , the blocking molecule is completely folded and no longer hinders the diffusion process, so that  $S$  is exactly the same as for unhindered

1 diffusion of  $x$ , namely

$$3 \quad -v = (F_s + F_f H(x - L)) \frac{\partial S}{\partial x} + k_B T \frac{\partial^2 S}{\partial x^2}, \quad (25)$$

5 subject to the boundary condition  $S = 0$  at  $x = 0$  and  $S = 0$  at  $x = l$ .

7 Notice that  $S(0, y)$  is the mean exit time starting from  $x = 0$  and  $y$ . However, to find the mean translocation time for secretion we must know something about the position of the previously secreted molecule when the secretion begins.

11 Suppose that immediately after the previous secretion, the trailing end  $y$  moves diffusively with probability distribution function  $p(y, t)$  where

$$15 \quad v p_t = -(F_f H(y - L + l) p)_y + k_B T p_{yy} \quad (26)$$

17 with  $p_y = 0$  at  $y = 0$  and  $p = 0$  at  $y = L$ . Suppose further that binding of the next secretant molecule is via a Poisson process with rate  $\lambda$ . Then, the distribution of locations  $\hat{y}$  at the beginning of the next secretion event is

$$21 \quad P(\hat{y}) = \int_0^\infty p(\hat{y}, t) \lambda e^{-\lambda t} dt. \quad (27)$$

23 If  $\tau$  is the mean translocation time for  $x$ , then the expected value of  $\tau$  is

$$27 \quad E(\tau) = \int_0^\infty P(\hat{y}) S(0, \hat{y}) d\hat{y}, \quad (28)$$

29 where  $S$  is the solution of the Eq. (24). A derivation of this equation is given in the Appendix.

31 The results (found by numerical determination of  $E(\tau)$  in Eq. (28)) are shown in Fig. 12 for parameter values given in Table 4. In this plot, the lower curve shows the mean unhindered translocation time (found by solving Eq. (25)), and the upper curve shows the hindered translocation time. Once again we see that there is a transition between unimpeded translocation and hin-

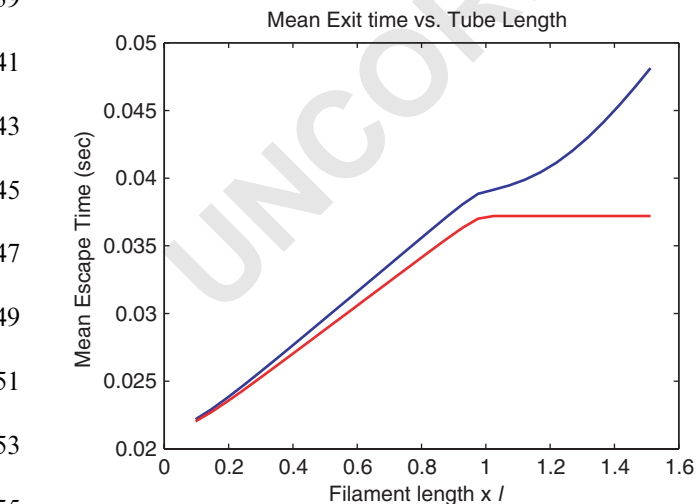


Fig. 12. Mean exit time for the two particle Fokker–Planck model.

Table 4  
Parameter values for Fig. 12

$D$	$10^{-10} \text{ cm}^2/\text{s}$	59
$\lambda$	10/s	61
$\frac{F_s}{v l}$	25/s	63
$\frac{F_f}{v l}$	20/s	65
$l$	75 nm	67

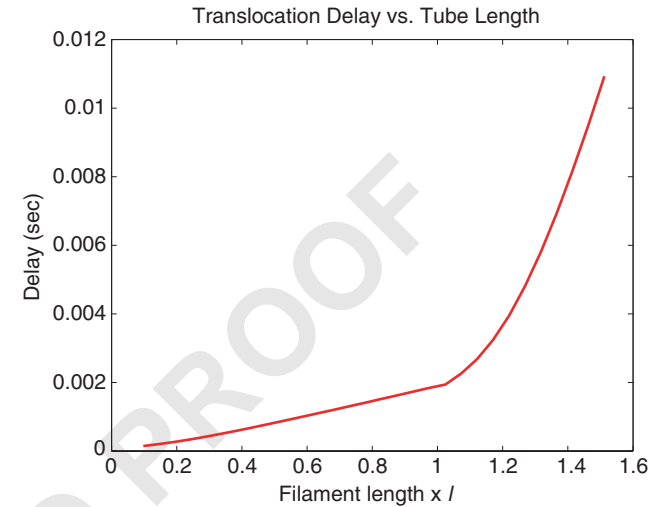


Fig. 13. Mean translocation delay for the two particle Fokker–Planck model.

33 dered translocation, that occurs at tube length  $L \sim l$ . The mean translocation delay, defined as the difference between the hindered and unhindered translocation times is shown in Fig. 13.

37 There are two differences between the Langevin model and the Fokker–Planck model that deserve explanation. First, notice that the delay for  $L < l$  is much smaller in Fig. 9 than in Fig. 13. This difference is due to the difference in the amplitude of diffusion in the two computations. In the deterministic limit  $D \rightarrow 0$ , there is no possibility that secretion is hindered if  $L < l$ . Second, in the Langevin model there is a noticeable plateau in the translocation time as a function of  $L$ , whereas in the Fokker–Planck model the translocation time is nearly linear in  $L$  for  $L < l$ . This difference in behavior is due entirely to the fact that molecules are modeled as springs in the Langevin model and as rigid rods in the Fokker–Planck model. In the limit that the spring constant becomes infinite, the translocation time for the Langevin model approaches a linear curve for  $L < l$ . The plateau behavior seen in Fig. 9 is due entirely to compression of the spring. In reality, this compression is probably quite small, so the plateau in Fig. 9 is probably an exaggeration compared to what occurs in the physical system.

#### 4. Hook length control

The proposed mechanism of hook length control is that FliK interacts with FlhB to change the secretion target of the secretion machinery. This interaction is thought to be by proteolytic activity of FliK that cleaves a portion of the FlhB molecule, thereby changing the secretion target. Once this cleavage takes place, FliK and FlgE can no longer be secreted, and secretion is restricted to a new class of molecules (including FliC, the constituent molecule for filaments). Our suggestion is that this interaction cannot occur if translocation is rapid, but it is promoted when translocation is delayed. In particular, we propose that if FliK secretion is accomplished by the normal ATP-ase and possibly some pulling from polymerization folding, then interaction with FlhB is prevented, while if secretion is delayed, then interaction with FlhB is possible. It could be that this interaction occurs simply because there is sufficient time, or it could be that FliK is able to sense a difference in mechanical forces between hindered and unhindered secretion. It is not known which, if any, of these is correct.

The simplest assumption is that the FliK–FlhB interaction is a Poisson process with rate  $k_{KB}$ . If  $T_d$ , the delay time, is the amount of time available for interaction, then the probability of interaction is taken to be

$$P(\text{FliK–FlhB interaction}) = 1 - \exp(-k_{KB}T_d). \quad (29)$$

Since this delay time is a function of the length of the hook  $T_d = T_d(L)$ , we can express this more succinctly as

$$P(\text{FliK–FlhB interaction}) = 1 - \exp(-k_{KB}T_d(L)) = F(L). \quad (30)$$

The hook grows by discrete steps each time a FlgE molecule is secreted. However, at each growth step there

is the possibility that a molecule of FliK is secreted as well. (Here we ignore the possibility that more than one FliK molecule might be secreted after a growth step.) We suppose that the probability of secreting a FliK molecule is  $p_K$ , and depends on the relative availability of FlgE and FliK. Thus, the probability of secretion of FliK and its interaction with FlhB at length  $L$  is

$$P(\text{FliK–FlhB secretion/interaction}) = p_K F(L), \quad (31)$$

and the probability that there is no interaction at length  $L$  is

$$P(\text{no interaction}) = p_K(1 - F(L)) + (1 - p_K) = 1 - p_K F(L). \quad (32)$$

The probability that the first (and therefore the only) interaction occurs at length  $L_k$  is

$$P(\text{first interaction}) = p_K F(L_k) \prod_{j=1}^{k-1} (1 - p_K F(L_j)), \quad (33)$$

where  $L_k = \frac{k}{\beta}$ .

To be specific, we suppose that the time available for interaction is the translocation delay time and is depicted in Fig. 14. For this we used the functional representation

$$k_{KB}T_d(L) = \frac{A}{2} \left( L + \frac{1}{a} \ln \left( \frac{\cosh(a(L - L_0))}{\cosh(aL_0)} \right) \right), \quad (34)$$

with  $L_0 = 46$ ,  $a = 0.16$ ,  $A = 0.26$ .

For this function there is a transition at approximately  $L = 45$  nm. This was chosen based on the guess that unfolded monomer is 75–85 nm long and the width of the basal body is  $\sim 35$  nm. With this as our assumed probability of success, the resulting probability distribution function for hooks lengths varies depending on the FliK secretion probability  $p_K$ . Several examples are shown in Fig. 15 (the cumulative distribution function) and Fig. 16 (the probability density function). In (a) is

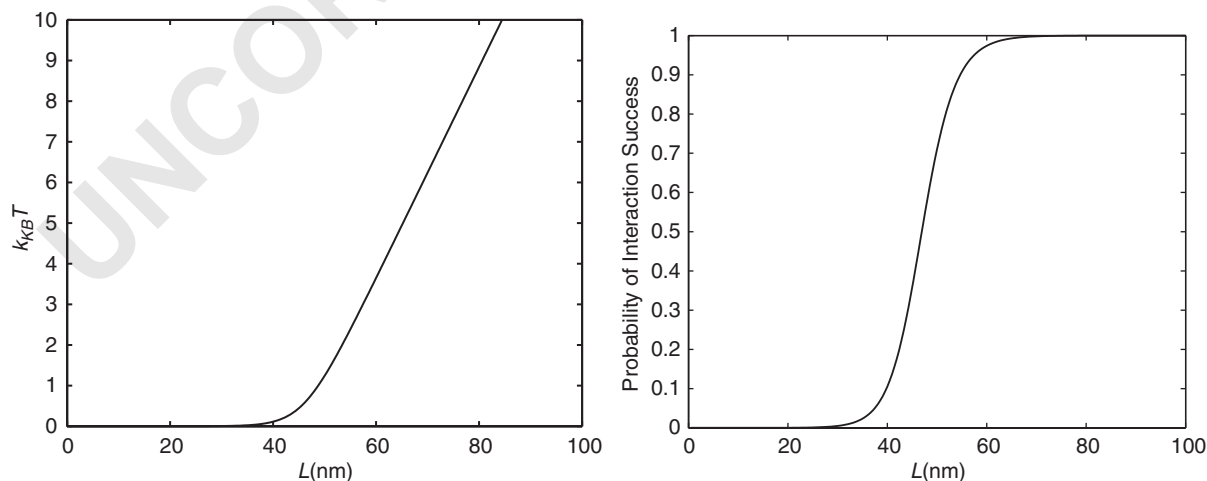


Fig. 14. Interaction time (left) and probability of interaction success (right) as functions of hook length  $L$ .

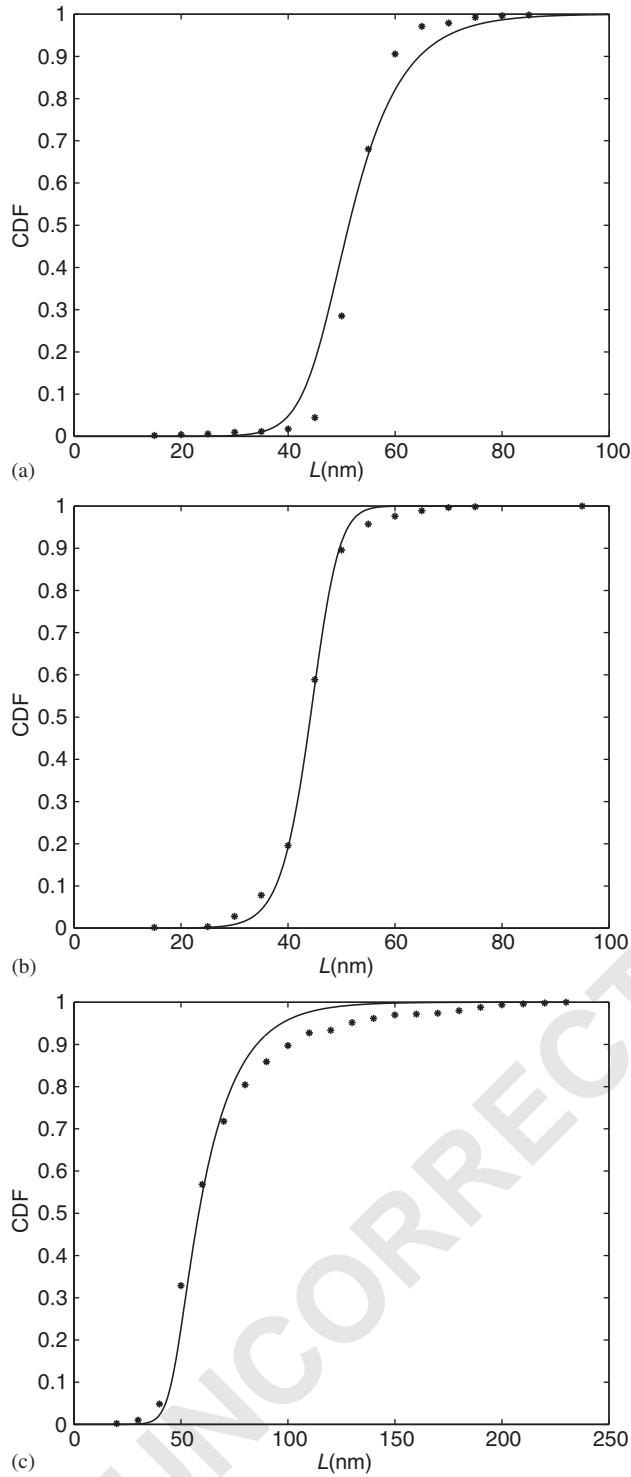


Fig. 15. Cumulative distribution function for hook length as a function of (continuous)  $L$  for (a) wild type ( $p = 0.06$ ), (b) when FliK is overproduced ( $p = 0.284$ ), and (c) when FliK is underproduced ( $p = 0.028$ ).

shown the distribution when  $p_K = 0.06$ . This distribution has mean  $54 \pm 9$  nm, and is in reasonable agreement with the data shown in Fig. 2(a) (represented by asterisks).  $p_K = 0.06$  corresponds to about 7 molecules

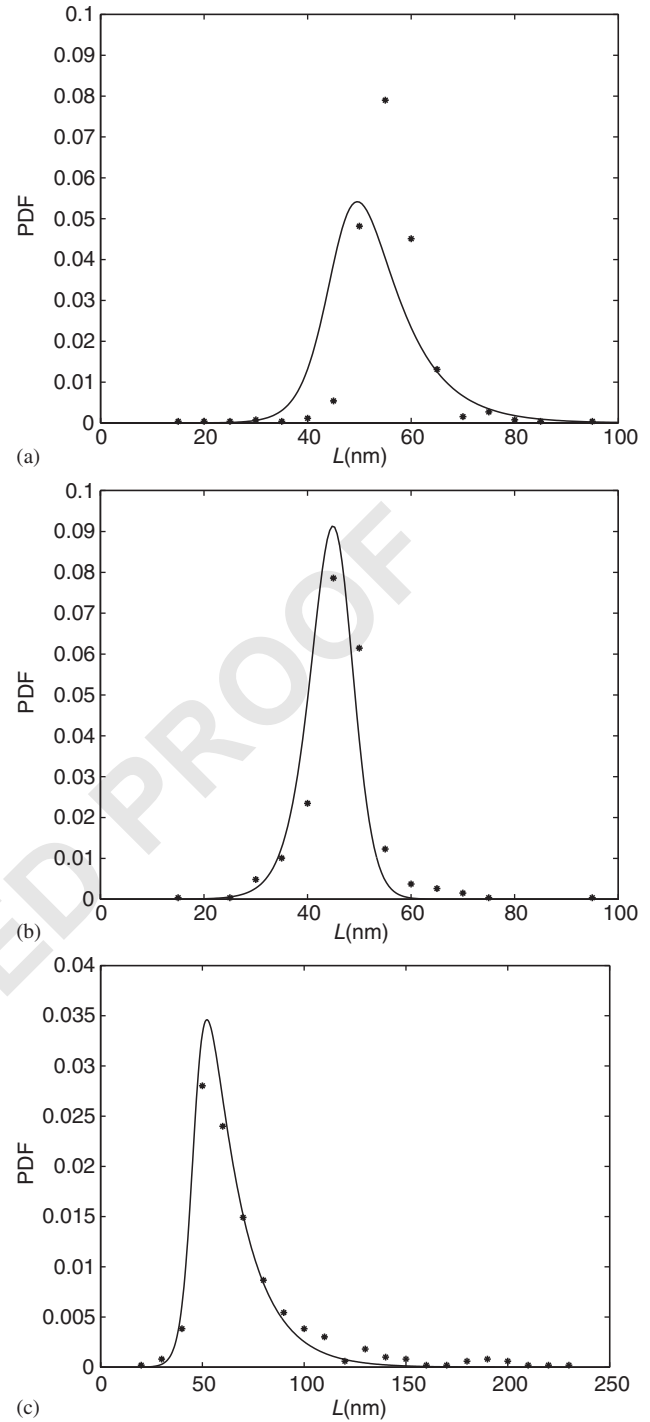


Fig. 16. Probability density function for hook length as a function of (continuous)  $L$  for (a) wild type ( $p = 0.06$ ), (b) when FliK is overproduced ( $p = 0.284$ ), and (c) when FliK is underproduced ( $p = 0.028$ ).

of secreted FliK per hook, which is apparently in the right ballpark. (In Muramoto et al. (1998), it was estimated that 40–80 molecules of FliK are used per cell to make about 8 flagellar motors.) In (b) is shown the

distribution when FliK is overproduced with  $p_K = 0.284$ . This distribution has mean  $44 \pm 5$  nm, which also agrees reasonably well with the data shown in Fig. 2(b). Finally, with  $p_K = 0.028$ , the distribution is as shown in (c), again giving reasonable agreement with the data shown in Fig. 2(c).

## 5. Discussion

Here we have presented models of monomer secretion and diffusion showing that there is a switch between secretion-limited growth and diffusion-limited growth that may be detected by the secretant FliK. This switch may be the signal that terminates the growth of hooks and initiates the secretion of other proteins required for filaments.

From these models it is possible to give a more detailed explanation of how the translocation time switch works. Every monomer is exposed to three forces, the force of the ATP-ase during secretion, the force of folding during polymerization and the random force of diffusion. When the tube is short, a monomer can begin to fold even before secretion is complete. When the tube is longer than the length of a monomer, there is a period of time during which the only force on a monomer in the tube is random diffusion. Once the monomer diffuses to the polymerizing end it is quickly pulled out of the tube by folding. However, while it is in the tube, it will hinder the free translocation of a subsequently secreted monomer. As a result the length at which this switch occurs is related to the length of the monomer in the tube, not the length of the monomer that is being secreted. This suggests that the wild type length of hooks is related to the unfolded length of FlgE, rather than the unfolded length of FliK.

While these results are encouraging, we are a long way from verifying that this is the mechanism by which hook length is determined. This model is able to reproduce the data shown in Fig. 2, but it does not provide an explanation for the data presented in Makishima et al. (2001). In that paper the authors reported finding a number of mutant strains of *Salmonella* with two classes of short hooks, a group with  $\sim 25$  nm hooks and a group with  $\sim 45$  nm hooks. All of the mutations were to proteins involved in the construction of a structure beneath the flagellar basal body called the C ring (C for cytoplasmic). The C ring is known to be important to the motor function of the flagellar motor, but it also interacts (in unknown ways) with the export apparatus. It is possible that changes to the C ring structure could interfere with export apparatus in such a way as to alter the transport of FliK, leading to changes in the length detection mechanism. However, there is as yet no mechanistic proposal for how this might work.

In Koroyasu et al. (2003) it was found that in a large population of FliK mutants there was a peak in the population of polyhooks at 55 nm, leading these authors to conclude that the length of hooks is determined by some mechanism independent of FliK. We contend that their conclusion is not justified, but results from a misinterpretation of their data.

To understand this, suppose that  $U(L, t)$  is the hook length density in a growing cell population. We suppose that individual hooks grow at a rate  $v(L)$ , a function of hook length  $L$ . The conservation law for  $U$  is (Koroyasu et al., 2003)

$$\frac{\partial U}{\partial t} + \frac{\partial}{\partial L}(v(L)U) = 0. \quad (35)$$

Suppose further that the total cell population  $N(t)$  is growing exponentially according to the growth law

$$\frac{dN}{dt} = GN. \quad (36)$$

We set  $U = uN$  (so that  $u$  is the per capita hook density), and determine that

$$\frac{\partial u}{\partial t} + Gu + \frac{\partial}{\partial L}(v(L)u) = 0. \quad (37)$$

If this process has been going on for some time and if new hooks (i.e. hooks of length  $L = 0$ ) are initiated at a rate proportional to the population growth rate, then  $u$  should approach a steady distribution  $u(L)$ , which satisfies the ordinary differential equation

$$\frac{d}{dL}(v(L)u) = -Gu. \quad (38)$$

This relationship can be used to determine  $v(L)$  from  $u$ . However, rewriting Eq. (38) as

$$\frac{u'}{u} = -\frac{v'}{v} - \frac{G}{v}, \quad (39)$$

we see that if  $v'(L) < 0$ , it is possible for the distribution  $u$  to have a local maximum. This local maximum occurs at that value of  $L$  at which  $v' = -G$ . In other words, the location of the maximum of the distribution of hook lengths  $u$  is determined by the growth rate of the cell population and the fact that  $v(L)$  is a decreasing function of  $L$ , not by any length selection mechanism. Thus, if it were possible to independently vary the population growth rate  $G$  without changing  $v(L)$ , the growth rate of hooks, one could freely adjust the location of the maximal population of hook lengths.

## Acknowledgements

This research was supported in part by NSF Grant DMS-0211366. Special thanks to Bob Guy and Tom Robbins for stimulating discussions, and to Kelly Hughes for his answers to my many questions.

## Appendix

The purpose of this appendix is to provide a derivation of Eq. (28).

As was stated above, we suppose that immediately after a secretion event, the trailing end of the secreted molecule  $y$  moves diffusively with probability distribution function  $p(y, t)$  where

$$v p_t = -(F_f H(y - L + l) p)_y + k_B T p_{yy} \quad (40)$$

with  $p_y = 0$  at  $y = 0$  and  $p = 0$  at  $y = L$ . Suppose further that binding of the next secretant molecule is via a Poisson process with binding rate  $\lambda$ . Then, the distribution of locations  $\hat{y}$  at which the next secretion begins is

$$P(\hat{y}) = \int_0^\infty p(\hat{y}, t) \lambda e^{-\lambda t} dt. \quad (41)$$

Now suppose that  $p(x', y', t | x, y, 0)$  is the probability density of the two-component ‘‘particle’’ being at position  $x', y'$  at time  $t$  having started at time  $t = 0$  at position  $x, y$ . The probability that the particle is somewhere in  $R$  at time  $t$  is

$$G(x, y, t) = \int_R p(x', y', t | x, y, 0) dx' dy', \quad (42)$$

where  $G(x, y, 0) = 1$ . If  $T$  is the time at which the particle leaves  $R$ , then

$$\text{Prob}(T \geq t) = G(x, y, t) = - \int_t^\infty G_t(x, y, s) ds, \quad (43)$$

a function of  $x$  and  $y$ . It follows that  $-G_t(x, y, t)$  is the probability density function for the random variable  $T$ . Therefore, the expected value of  $T$  is

$$\begin{aligned} S \equiv \langle T \rangle &= - \int_0^\infty t G_t(x, y, t) dt \\ &= \int_0^\infty G(x, y, t) dt. \end{aligned} \quad (44)$$

It also follows from Eq. (42) that

$$G_t(x, y, t) = \int_R p_t(x', y', t | x, y, 0) dx' dy'. \quad (45)$$

Since this is a time autonomous process,  $p(x', y', t | x, y, 0) = p(x', y', 0 | x, y, -t)$ . Thus,  $G(x, y, t)$  satisfies the partial differential equation

$$\begin{aligned} v G_t &= v \int_R -p_t(x', y', 0 | x, y, -t) dx' dy' \\ &= \left( \begin{array}{c} F_s \\ F_f H(y - L + l) \end{array} \right) \cdot \nabla G + k_b T \nabla^2 G, \end{aligned} \quad (46)$$

(the backward Kolmogorov equation). Integrating Eq. (46) with respect to time, we find the (24) for  $S(x, y)$ .

Now, we let  $\tau$  be the translocation time. Thus, we start the process at  $x = 0$  with the distribution of  $y$  locations  $P(y)$ . Since  $G(0, \hat{y}, t)$  is the probability that  $\tau \geq t$  given that the process is started at  $x = 0$  and  $y = \hat{y}$ , it follows that

$$\begin{aligned} P(\tau \geq t) &= \int_0^\infty P(\hat{y}) G(0, \hat{y}, t) d\hat{y} \\ &= - \int_0^\infty P(\hat{y}) \int_t^\infty G_t(0, \hat{y}, t) dt d\hat{y}. \end{aligned} \quad (47)$$

Thus, the expected value of  $\tau$  is

$$\begin{aligned} E(\tau) &= - \int_0^\infty \int_0^\infty P(\hat{y}) t G_t(0, \hat{y}, t) dt d\hat{y} \\ &= \int_0^\infty P(\hat{y}) \int_0^\infty G(0, \hat{y}, t) dt d\hat{y} \\ &= \int_0^\infty P(\hat{y}) S(0, \hat{y}) d\hat{y}, \end{aligned} \quad (48)$$

where  $S$  is the solution of Eq. (24).

## References

- Bird, R.B., Curtiss, C.F., Armstrong, R.C., Hassager, O., 1987. Dynamics of Polymeric Liquids, vol. 2, second ed. Wiley, New York
- Gardiner, C.W., 1985. Handbook of Stochastic Methods, second ed. Springer, Berlin.
- Hughes, K.T., Aldridge, P.D., 2001. Putting a lid on it. Nat. Struct. Biol. 8, 96–97.
- Iino, T., 1974. Assembly of *Salmonella* flagellin in vitro and in vivo. J. Supramol. Str. 2, 372–384.
- Koroyasu, S., Yamazoto, M., Hirano, T., Aizawa, S.-I., 2003. Kinetic analysis of the growth rate of the flagellar hook in *Salmonella typhimurium* by the population balance method. Biophys. J. 74, 436–443.
- Kutsukake, K., Ohya, Y., Iino, T., 1990. Transcriptional analysis of the flagellar regulon of *Salmonella typhimurium*. J. Bacteriol. 172, 741–747.
- Macnab, R.M., 2003. How bacteria assemble flagella. Ann. Rev. Microbiol. 57, 77–100.
- Makishima, S., Komoriya, K., Yamaguchi, S., Aizawa, S.-I., 2001. Length of the flagellar hook and the capacity of the type III export apparatus. Science 291, 2411–2413.
- Minamino, T., Gonzalez-Pedrajo, B., Yamaguchi, K., Aizawa, S.I., Macnab, R.M., 1999. FliK, the protein responsible for flagellar hook length control in *Salmonella*, is exported during hook assembly. Mol. Microbiol. 34, 295–304.
- Minamino, T., Macnab, R.M., 2000. Interactions among components of the *Salmonella* flagellar export apparatus and its substrates. Mol. Microbiol. 19, 1–5.
- Muramoto, K., Makishima, S., Aizawa, S.-I., Macnab, R.M., 1998. Effect of cellular level of FliK on flagellar hook and filament assembly in *Salmonella typhimurium*. J. Mol. Biol. 277, 871–882.
- Yonekura, K., Maki-Yonekura, S., Namba, K., 2003. Complete atomic model of the bacterial flagellar filament by electron cryomicroscopy. Nature 424, 643–650.